

## *Invited Review*

# Thermodynamic Investigation of Phase Equilibria in Metal Carbonate– Water–Carbon Dioxide Systems

Wolfgang Preis\* and Heinz Gamsjäger

Institut für Physikalische Chemie, Montanuniversität Leoben, Franz-Josef-Strasse 18,  
A-8700 Leoben, Austria

**Summary.** Solubility measurements as a function of temperature have been shown to be a powerful tool for the determination of thermodynamic properties of sparingly-soluble transition metal carbonates. In contrast to calorimetric methods, such as solution calorimetry or drop calorimetry, the evaluation of solubility data avoids many systematic errors, yielding the enthalpy of solution at 298.15 K with an estimated uncertainty of  $\pm 3 \text{ kJ} \cdot \text{mol}^{-1}$ . A comprehensive set of thermodynamic data for otavite ( $\text{CdCO}_3$ ), smithsonite ( $\text{ZnCO}_3$ ), hydrozincite ( $\text{Zn}_5(\text{OH})_6(\text{CO}_3)_2$ ), malachite ( $\text{Cu}_2(\text{OH})_2\text{CO}_3$ ), azurite ( $\text{Cu}_3(\text{OH})_2(\text{CO}_3)_2$ ), and siderite ( $\text{FeCO}_3$ ) was derived. Literature values for the standard enthalpy of formation of malachite and azurite were disproved by these solubility experiments, and revised values are recommended. In the case of siderite, data for the standard enthalpy of formation given by various data bases deviate from each other by more than  $10 \text{ kJ} \cdot \text{mol}^{-1}$  which can be attributed to a discrepancy in the auxiliary data for the  $\text{Fe}^{2+}$  ion. A critical evaluation of solubility data from various literature sources results in an optimized value for the standard enthalpy of formation for siderite. The *Davies* approximation, the specific ion-interaction theory, and the *Pitzer* concept are used for the extrapolation of the solubility constants to zero ionic strength in order to obtain standard thermodynamic properties valid at infinite dilution,  $T = 298.15 \text{ K}$ , and  $p = 10^5 \text{ Pa}$ . The application of these electrolyte models to both homogeneous and heterogeneous (solid-solute) equilibria in aqueous solution is reviewed.

**Keywords.** Thermodynamics; Solubility; Transition metals; Carbonate.

## Introduction

The thermodynamic properties of transition metal carbonates play a major role for a better understanding of a wide variety of geochemical and industrial processes involving equilibria between solid carbonates and aqueous solutions. The total concentration of transition metals in carbonate-bearing natural waters is predominantly determined by the solubilities of the respective hydroxides, oxides,

\* Corresponding author. E-mail: gamsjaeg@unileoben.ac.at

hydroxide carbonates, and neutral carbonates [1]. The thermodynamic modeling of dissolution or precipitation of sparingly-soluble metal carbonates may serve as an important tool for the prediction of the concentrations of transition metals in mine pit lakes [2]. A careful determination of thermodynamic data of metal carbonates is an essential prerequisite for the geochemical modeling of the release of trace elements from waste repositories [3].

In general, the standard *Gibbs* free energy of formation of a solid compound can be obtained from the determination of equilibrium constants or the measurement of the *emf* (electromotive force) of an appropriate electro-chemical cell. In the case of sparingly-soluble metal carbonates the careful determination of the solubility constant has led to reliable values for the standard *Gibbs* free energies of formation [4–11]. An alternative path for the determination of this quantity is the application of electrochemical cells using carbonate electrodes of the third kind without liquid junction [12–14].

The standard enthalpy of formation,  $\Delta_f H^\ominus$ , of metal carbonates can be measured by application of both calorimetric and equilibrium methods. Direct measurements of the enthalpy of solution by means of solution calorimeters operating at moderate temperatures (293–323 K) enable the determination of the enthalpy of formation of the mineral phase [15–18]. In addition, the application of drop calorimetry [19–21], drop solution calorimetry [22–24], and DSC (differential scanning calorimetry) [10, 11] has been reported. By using adequate thermodynamic cycles,  $\Delta_f H^\ominus$  was calculated from the directly determined enthalpy change associated with (i) the drop of the specimen into the hot calorimeter and subsequent decomposition regarding drop calorimetry, or (ii) the drop of the sample and subsequent dissolution in molten lead borate glasses concerning drop solution calorimetry.

Alternatively, the enthalpy of solution and the enthalpy of decomposition can be obtained from the temperature dependence of the solubility constant [9–11] and the decomposition pressure [25, 26], respectively. It should be noted that the decarbonation measurements at elevated temperatures are difficult to evaluate, since the compressibility of solid carbonates as well as the fugacities of carbon dioxide at extremely high pressures are rather uncertain [25]. If  $\Delta_f H^\ominus$  is derived from solubility measurements at various temperatures, a powerful electrolyte theory is necessary for the extrapolation of the solubility constants to infinite dilution.

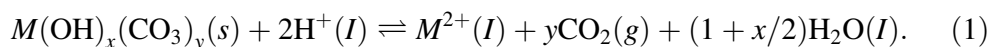
The standard entropy of the solid carbonate can be calculated from the entropy of solution obtained from solubility measurements as a function of temperature. However, the most accurate and precise method for the determination of the standard entropy of a solid phase is the integration of the heat capacity function from 0 to 298.15 K. Low-temperature measurements of the heat capacity have been carried out for a number of transition metal carbonates, resulting in highly reliable values for the standard entropy [19, 27–29].

It is the aim of this work to derive an internally consistent set of thermodynamic properties, *i.e.* standard enthalpy of formation, standard entropy, and standard *Gibbs* free energy of formation, for the following transition metal carbonates: otavite ( $\text{CdCO}_3$ ), smithsonite ( $\text{ZnCO}_3$ ), hydrozincite ( $\text{Zn}_5(\text{OH})_6(\text{CO}_3)_2$ ), malachite ( $\text{Cu}_2(\text{OH})_2\text{CO}_3$ ), azurite ( $\text{Cu}_3(\text{OH})_2(\text{CO}_3)_2$ ), and siderite ( $\text{FeCO}_3$ ). Basically, the

thermodynamic quantities are derived from solubility measurements as a function of temperature and ionic strength. Details on experimental procedures have been given elsewhere [4, 7–10, 30–32] and need not to be discussed further in this contribution. The application of different models for the extrapolation of the solubility constants to zero ionic strength is reviewed. This extrapolation allows the derivation of standard thermodynamic data valid at infinite dilution,  $T = 298.15\text{ K}$ , and  $p = 10^5\text{ Pa}$ . The solubility data are evaluated with the help of the optimization routine of ChemSage [33]. Whereas the standard entropies of the solid carbonates are generally given by low-temperature measurements of the heat capacity, the standard *Gibbs* free energy of formation as well as the standard enthalpy of formation are obtained from the solubility measurements. In the case of hydrozincite, no direct determination of the standard entropy has been reported so far. Thus, this quantity is likewise derived from the temperature dependence of the solubility constant. Additionally, all results will be compared with a large number of thermodynamic investigations published in literature.

### Theoretical Aspects

The dissolution of a sparingly-soluble metal(II) carbonate  $M(\text{OH})_x(\text{CO}_3)_y(s)$  in an aqueous medium of a certain ionic strength  $I$  can be expressed as



Owing to the charge balance equation, the relation  $x + 2y = 2$  must be fulfilled. The solubility constant valid at a given temperature  $T$  and ionic strength  $I$  can be written as

$$\log {}^*K_{ps0}^I = \log ([M^{2+}]/m^\ominus)(p(\text{CO}_2)/p^\ominus)^y([H^+]/m^\ominus)^{-2} \quad (2)$$

where the square brackets refer to the molalities of the respective species in the aqueous phase and  $p(\text{CO}_2)$  denotes the partial pressure of carbon dioxide. The standard molality and the standard pressure are defined as  $m^\ominus = 1\text{ mol} \cdot \text{kg}^{-1}$  and  $p^\ominus = 10^5\text{ Pa}$ , respectively. According to Eq. (2), the solubility of the solid carbonate is determined by three parameters: the partial pressure of carbon dioxide, the molality of the metal ions, and the  $p[H]$ . The square brackets of  $p[H]$  indicate that with the calibration system used  $\text{H}^+$  ion molalities were measured. Usually, the  $\text{CO}_2$  pressure is maintained constant during the solubility experiments, the molality of the metal ions can be determined by complexometric titrations with *EDTA*, and the  $p[H]$  of the aqueous solution in equilibrium with the solid carbonate and the gas phase is obtained from potentiometric measurements.

By fixing the ionic strength,  $I$ , of the solvent (usually aqueous  $\text{NaClO}_4$  solutions) at a constant value, reliable equilibrium constants  $\log {}^*K_{ps0}^I$  can be obtained. These solubility constants are extrapolated to zero ionic strength,  $\log {}^*K_{ps0}^0$ , by calculating the ionic strength dependence of the individual activity coefficients ( $\gamma(M^{2+})$ ,  $\gamma(\text{H}^+)$ ) as well as the activity of water,  $a(\text{H}_2\text{O})$ :

$$\log {}^*K_{ps0}^0 = \log {}^*K_{ps0}^I + \log \gamma(M^{2+}) - 2\log \gamma(\text{H}^+) + (1 + x/2)\log a(\text{H}_2\text{O}). \quad (3)$$

The activity of water is correlated to the osmotic coefficient  $\phi$  by Eq. (4) [34], where  $M_{\text{H}_2\text{O}}$  and  $\sum m_i$  are the molar mass of water and the sum over the molalities

of all species in solution.

$$\phi = -\frac{\ln a(\text{H}_2\text{O})}{M_{\text{H}_2\text{O}} \sum m_i} \quad (4)$$

The individual activity coefficients of the solutes in a multicomponent aqueous phase are related to the osmotic coefficient (activity of water) by the *Gibbs-Duhem* equation [35]:

$$-\sum m_i d\phi - (\phi - 1) \sum dm_i + \sum (m_i d \ln \gamma_i) = 0. \quad (5)$$

When solubility experiments are performed in perchlorate media of fairly high ionic strengths ( $I \geq 0.20 \text{ mol} \cdot \text{kg}^{-1} \text{ NaClO}_4$ ), precise *pH* values can be guaranteed. We have applied the *Davies* approximation [36], the specific ion-interaction theory [37], and the *Pitzer* equations [38] to take into account the solute-solvent interactions at such high ionic strengths. In the following discussion of electrolyte models, quantity algebra was sacrificed in order to improve readability.

#### *Davies approximation*

In general, the *Davies* approximation is useful for the prediction of the ionic strength dependence of the mean activity coefficient of strong electrolyte solutions up to molalities around  $0.1\text{--}0.2 \text{ mol} \cdot \text{kg}^{-1}$ . The individual activity coefficient  $\gamma_i$  of an ionic species in aqueous solution is given by

$$\log \gamma_i = -Az_i^2 \left( \frac{\sqrt{I}}{1 + \sqrt{I}} - 0.3I \right) \quad (6)$$

with  $A$  and  $z_i$  denoting the *Debye-Hückel* parameter and the ionic charge number, respectively. In accordance with the *Gibbs-Duhem* relation (Eq. (5)), the osmotic coefficient reads

$$\phi = 1 - \frac{\ln(10)A}{\sum m_i} \left( 2 + 2\sqrt{I} - \frac{2}{1 + \sqrt{I}} - 4\ln(1 + \sqrt{I}) - 0.3I^2 \right). \quad (7)$$

If a 1–1 electrolyte, such as  $\text{NaCl}$  or  $\text{NaClO}_4$ , is employed to fix the ionic strength, the extrapolation of the solubility constant to infinite dilution can be expressed as

$$\log {}^*K_{ps0}^0 = \log {}^*K_{ps0}^I - 2A \left( \frac{\sqrt{I}}{1 + \sqrt{I}} - 0.3I \right) - (1 + x/2) \frac{2I\phi M_{\text{H}_2\text{O}}}{\ln(10)}, \quad (8)$$

where  $\phi$  is given by

$$\phi = 1 - \frac{\ln(10)A}{I} \left( 1 + \sqrt{I} - \frac{1}{1 + \sqrt{I}} - 2\ln(1 + \sqrt{I}) \right) + \frac{A\ln(10)}{2} 0.3I. \quad (9)$$

It should be mentioned that the *Davies* formalism is an extension of the *Debye-Hückel* limiting law without any individual interaction parameters.

#### *Specific ion-interaction theory*

The specific ion-interaction theory is likewise based on the *Debye-Hückel* limiting law. However, individual ion-interaction parameters are introduced which enable

the calculation of activity coefficients up to ionic strengths of  $3\text{--}4\text{ mol}\cdot\text{kg}^{-1}$ . This concept was originally introduced by *Brønsted* [39, 40], *Guggenheim* [41], and *Scatchard* [42]. *Grenthe et al.* [37] published many examples for the efficiency of this formalism with respect to homogeneous equilibria in media of constant ionic strength. The individual activity coefficient of an ionic species is defined as

$$\log \gamma_i = -\frac{Az_i^2\sqrt{I}}{1 + 1.5\sqrt{I}} + \sum \varepsilon(i,j)m_j \quad (10)$$

where only interaction coefficients  $\varepsilon(i, j)$  between ions of opposite charges are considered. In accordance with the traditional *Setchenov* equation the activity coefficient of uncharged species  $\gamma_k$  reads [37]

$$\log \gamma_k = \sum \varepsilon(k,j)m_j \quad (11)$$

where only interactions between the neutral species and ions are taken into account. The osmotic coefficient can be written as [37]

$$\phi = 1 - \frac{2\ln(10)A}{1.5^3 \sum m_i} \left( 1 + \sqrt{I} - \frac{1}{1 + \sqrt{I}} - 2\ln(1 + \sqrt{I}) \right) + \frac{\ln(10)}{2 \sum m_i} \sum_i \sum_j \varepsilon(i,j)m_i m_j \quad (12)$$

In the case of solutions of 1–1 electrolytes ( $NX$ ) serving as the inert ionic medium, the extrapolation of  $\log^* K_{ps0}^I$  to zero ionic strength is given by

$$\begin{aligned} \log^* K_{ps0}^0 &= \log^* K_{ps0}^I - \frac{2A\sqrt{I}}{1 + 1.5\sqrt{I}} \\ &\quad + (\varepsilon(M^{2+}, X^-) - 2\varepsilon(H^+, X^-))I - (1 + x/2) \frac{2I\phi M_{\text{H}_2\text{O}}}{\ln(10)}, \end{aligned} \quad (13)$$

with the osmotic coefficient  $\phi$  being

$$\phi = 1 - \frac{A\ln(10)}{1.5^3 I} \left( 1 + 1.5\sqrt{I} - \frac{1}{1 + 1.5\sqrt{I}} - 2\ln(1 + 1.5\sqrt{I}) \right) + \frac{\ln(10)}{2} \varepsilon(N^+, X^-)I. \quad (14)$$

The temperature dependence of the interaction parameters is given by the relation

$$\varepsilon(i,j) = \varepsilon(i,j; 298.15\text{ K}) + \frac{\partial \varepsilon(i,j)}{\partial T} (T - 298.15\text{ K}). \quad (15)$$

The values for  $\partial \varepsilon(i,j)/\partial T$  are based on the ionic strength dependence of the relative apparent molar enthalpy  ${}^\phi L$  of the pertinent strong electrolytes [37]

$${}^\phi L = \frac{3}{4}(\nu_+ + \nu_-) \frac{A_L |z_+ z_-|}{1.5^3 I} (t^2 - 4t + 2\ln t + 3) - \frac{2\ln(10)\nu_+ \nu_-}{\nu_+ z_+^2 + \nu_- z_-^2} RT^2 I \frac{\partial \varepsilon(i,j)}{\partial T} \quad (16)$$

where  $t = 1 + 1.5\sqrt{I}$  and  $A_L$  is the *Debye-Hückel* parameter for enthalpy [38]. The symbols  $\nu_+$ ,  $\nu_-$ ,  $z_+$ , and  $z_-$  denote the stoichiometric indices and charge numbers of the respective ions.

### Pitzer model

The *Pitzer* concept is even valid in the case of saturated solutions of highly-soluble strong electrolytes. In contrast to the former electrolyte theories a large number of individual interaction parameters is necessary. Single electrolyte solutions require at least the knowledge of three binary parameters. In the case of multicomponent systems, such as solubility equilibria of metal carbonates in constant ionic media, only an extensive set of binary and ternary interaction parameters allows a correct prediction of the solubility constant at ionic strengths above  $3 \text{ mol} \cdot \text{kg}^{-1}$  NaCl or  $\text{NaClO}_4$ .

The electrolyte models mentioned above are incorporated into the general *Gibbs* energy minimization program ChemSage [43] which permits a wide variety of equilibrium calculations in aqueous media. Furthermore, the optimization routine of ChemSage [33] allows the simultaneous evaluation of experimental data from different sources in order to obtain an internally consistent set of optimized thermodynamic constants.

A comparison between the specific ion-interaction theory and the *Pitzer* formalism is illustrated in Figs. 1 and 2. The mean activity coefficient and the osmotic coefficient are plotted as a function of molality of the 2–1 electrolyte  $\text{Zn}(\text{ClO}_4)_2$  at  $T = 298.15 \text{ K}$ . The *Pitzer* equations provide a perfect fit to the experimental data taken from Ref. [44] over the whole range of molality ( $0\text{--}4.3 \text{ mol} \cdot \text{kg}^{-1}$ ). The specific ion-interaction parameter  $\varepsilon(\text{Zn}^{2+}, \text{ClO}_4^-) = 0.36$  is obtained from a fit of Eqs. (10) and (12), respectively, to the experimental data from 0 to  $2.5 \text{ mol} \cdot \text{kg}^{-1}$ .

The application of the *Davies* approximation, the specific ion-interaction theory, and the *Pitzer* concept to the theoretical prediction of the ionic product

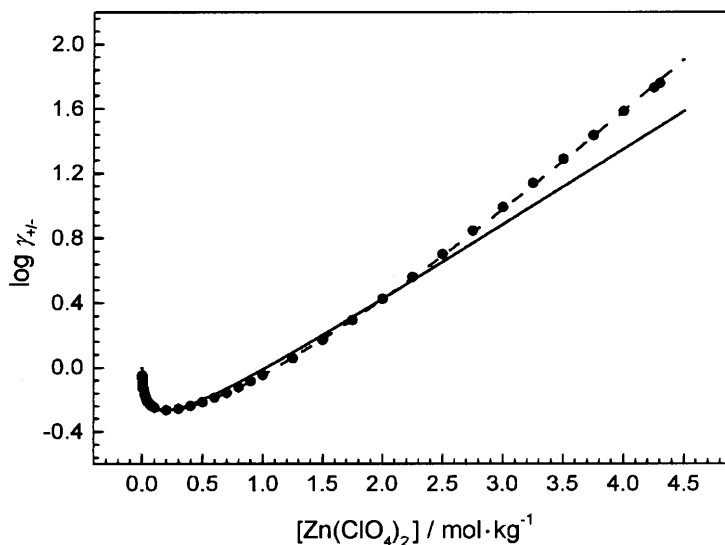


**Fig. 1.** Logarithm of the mean activity coefficient plotted vs. molality of  $\text{Zn}(\text{ClO}_4)_2$  at  $298.15 \text{ K}$ ; ●: Goldberg [44]; solid line: specific ion-interaction theory [37],  $\varepsilon(\text{Zn}^{2+}, \text{ClO}_4^-) = 0.36$ ; dashed line: *Pitzer* model [38]

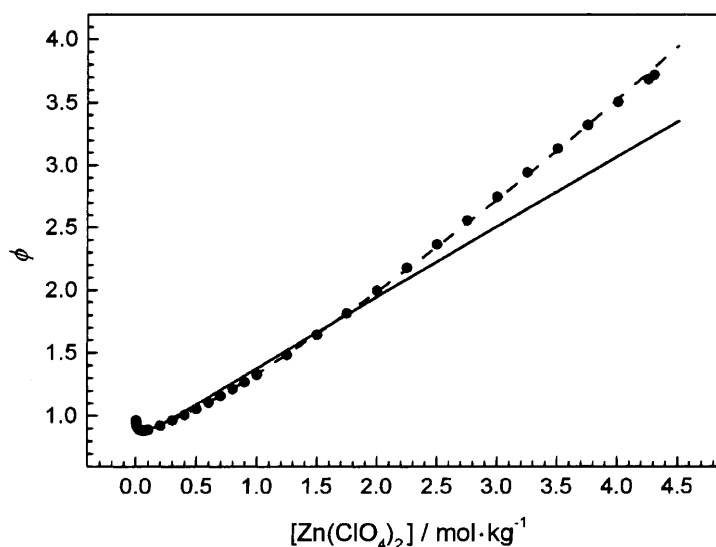


**Fig. 2.** Plot of the osmotic coefficient as a function of molality of  $\text{Zn}(\text{ClO}_4)_2$  at 298.15 K; ●: Goldberg [44]; solid line: specific ion-interaction theory [37],  $\epsilon(\text{Zn}^{2+}, \text{ClO}_4^-) = 0.36$ ; dashed line: Pitzer model [38]

of water,  $pK_w^I$ ,

$$pK_w^I = 14.00 + \log\gamma(\text{H}^+) + \log\gamma(\text{OH}^-) + \frac{2I\phi M_{\text{H}_2\text{O}}}{\ln(10)} \quad (17)$$

in solutions of sodium perchlorate and sodium chloride at 298.15 K is exemplified in Figs. 3 and 4, respectively. Again, the Pitzer equations allow a perfect description of the ionic strength dependence of  $pK_w^I$  by employing appropriate

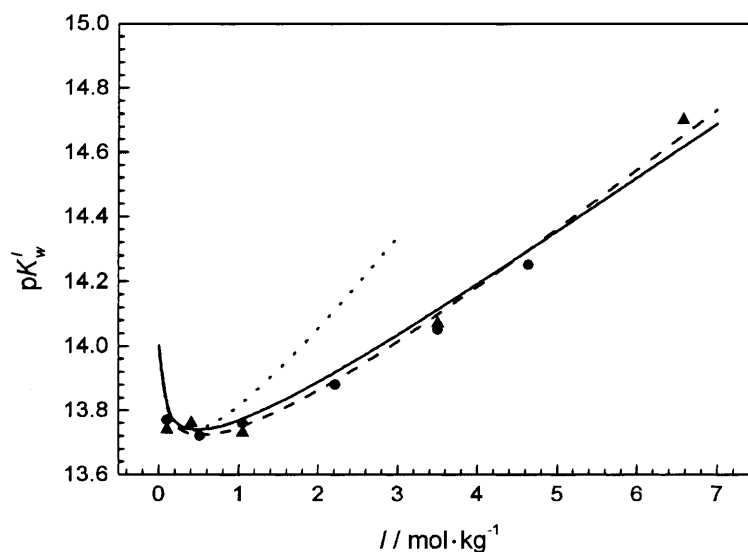


**Fig. 3.** Variation of  $pK_w^I$  with ionic strength  $I$  of  $\text{NaClO}_4$  at 298.15 K; ●: Fisher and Byé [45]; ▲: Carpéni *et al.* [46]; solid line: specific ion interaction theory [37]; dashed line: Pitzer model [38]; dotted line: Davies approximation [36]

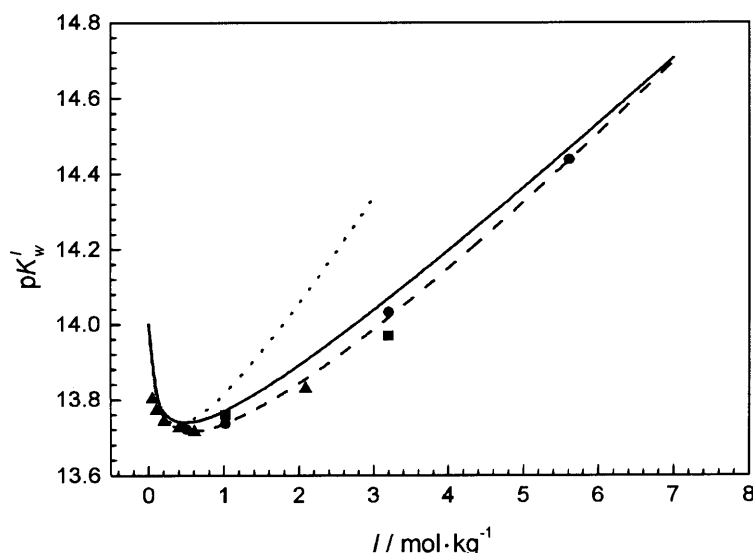


**Fig. 4.** Plot of  $pK_w^I$  vs. ionic strength  $I$  of NaCl at 298.15 K; ●: Kron *et al.* [47]; ▲: Sjöberg *et al.* [48]; ■: Näsänen and Meriläinen [49]; solid line: specific ion interaction theory [37]; dashed line: Pitzer model [38]; dotted line: Davies approximation [36]

ternary interaction parameters. Interestingly, the calculation of the ionic product of water in NaClO<sub>4</sub> solutions as a function of  $I$ , using the specific ion-interaction theory, is almost indistinguishable from the result of the Pitzer formalism (Fig. 3). In the case of NaCl the experimental data deviate from the calculated values employing the specific ion-interaction theory by less than 0.06  $\log K_w^I$  units (Fig. 4). The Davies formalism suffices to predict the ionic strength dependence of  $pK_w^I$  up to 1.0 mol·kg<sup>-1</sup> NaClO<sub>4</sub> or NaCl with a maximum deviation around 0.1  $\log K_w^I$ -units.

Apart from homogeneous equilibria (Figs. 3 and 4) the pertinent electrolyte theories are also applied to heterogeneous equilibria (Figs. 5 to 8) involving the dissolution of sparingly-soluble metal carbonates in constant ionic media consisting of NaClO<sub>4</sub> or NaCl.

The variations of the solubility constants of the transition metal carbonates CdCO<sub>3</sub> (Fig. 5) and ZnCO<sub>3</sub> (Fig. 6) with ionic strength  $I$  have been investigated at 298.15 K. The Davies formalism is valid up to an ionic strength of 1.0 mol·kg<sup>-1</sup> NaClO<sub>4</sub>. The specific ion-interaction theory provides a reasonable fit to the experimental data. Whereas the Pitzer model coincides perfectly with the experimental values in the case of cadmium carbonate (Fig. 5), a fairly large deviation occurs with respect to zinc carbonate especially at  $I = 3.0$  mol·kg<sup>-1</sup> NaClO<sub>4</sub> (Fig. 6). This discrepancy may be attributed to the lack of ternary interaction parameters for the system Zn(ClO<sub>4</sub>)<sub>2</sub>-NaClO<sub>4</sub>. It can be concluded that the specific ion-interaction theory leads to an even more accurate description of the ionic strength dependence of the solubility constant than the Pitzer model when essential ternary Pitzer parameters are unknown.

The application of the Pitzer equations and the specific ion-interaction theory to the modeling of the solubility of the alkaline earth metal carbonate calcite in



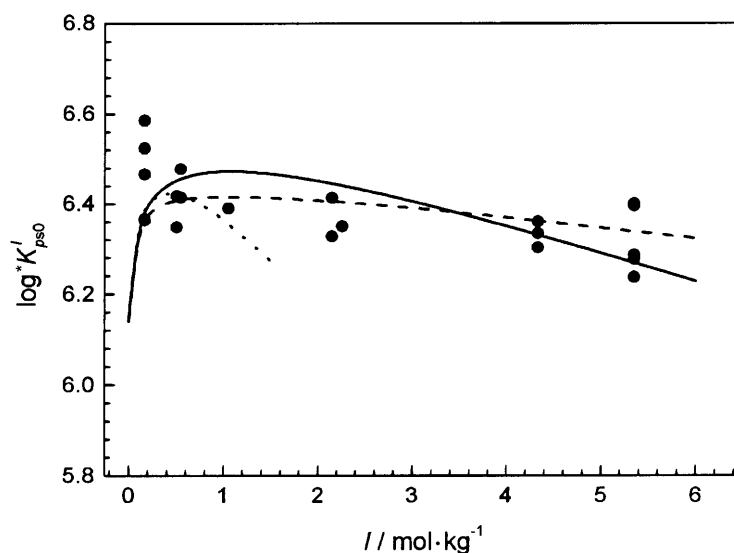


**Fig. 5.** Solubility constant of cadmium carbonate plotted vs. ionic strength at 298.15 K (inert electrolyte:  $\text{NaClO}_4$ );  $\log^* K_{ps0}^0 = 6.14 \pm 0.10$ ; ●: *Gamsjäger et al.* [9]; solid line: specific ion interaction theory [37]; dashed line: *Pitzer* model [38]; dotted line: *Davies* approximation [36]

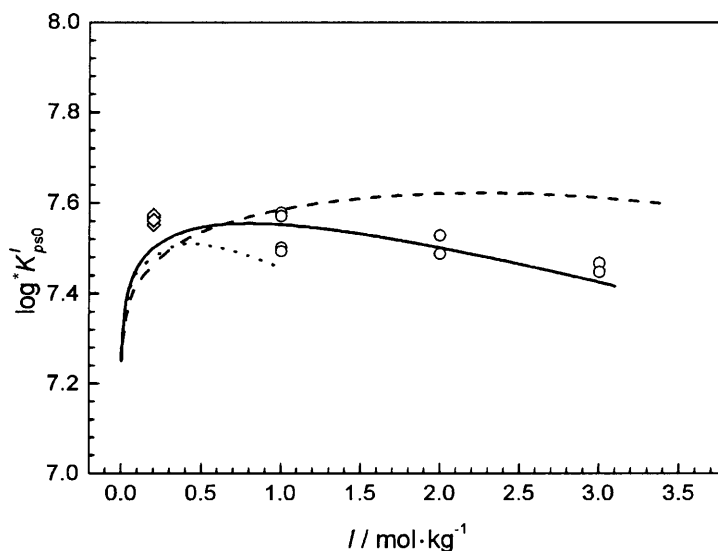


**Fig. 6.** Variation of  $\log^* K_{ps0}'$  of zinc carbonate with ionic strength at 298.15 K (inert electrolyte:  $\text{NaClO}_4$ );  $\log^* K_{ps0}^0 = 7.25 \pm 0.10$ ; ○: *Preis et al.* [10]; ◇: *Schindler et al.* [6]; solid line: specific ion interaction theory [37]; dashed line: *Pitzer* model [38]; dotted line: *Davies* approximation [36]

solutions of sodium chloride at three different temperatures (283.15, 298.15, and 333.15 K) is shown in Fig. 7. In addition, Fig. 8 represents the variation of the solubility constant of the rare earth metal carbonate lanthanite ( $\text{La}_2(\text{CO}_3)_3 \cdot 8\text{H}_2\text{O}$ ) with ionic strength at 298.15 K. All relevant ternary *Pitzer* parameters are sufficiently known, and the application of the *Pitzer* concept leads to an excellent

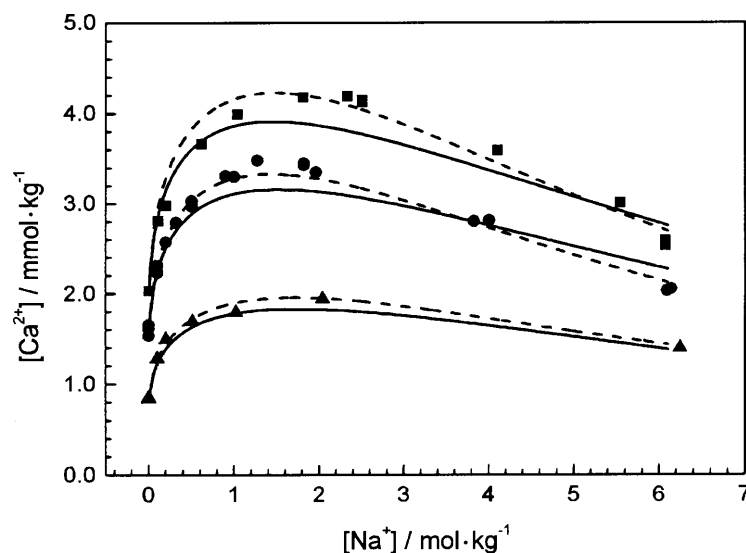


**Fig. 7.** Plot of solubility of calcite as a function of molality of sodium chloride; experimental data: Wolf *et al.* [50], ■:  $T = 283.15$  K,  $p(\text{CO}_2) = 0.0094$  bar, ●:  $T = 298.15$  K,  $p(\text{CO}_2) = 0.0092$  bar, ▲:  $T = 333.15$  K,  $p(\text{CO}_2) = 0.0078$  bar; solid line: specific ion interaction theory [37]; dashed line: Pitzer model [38]

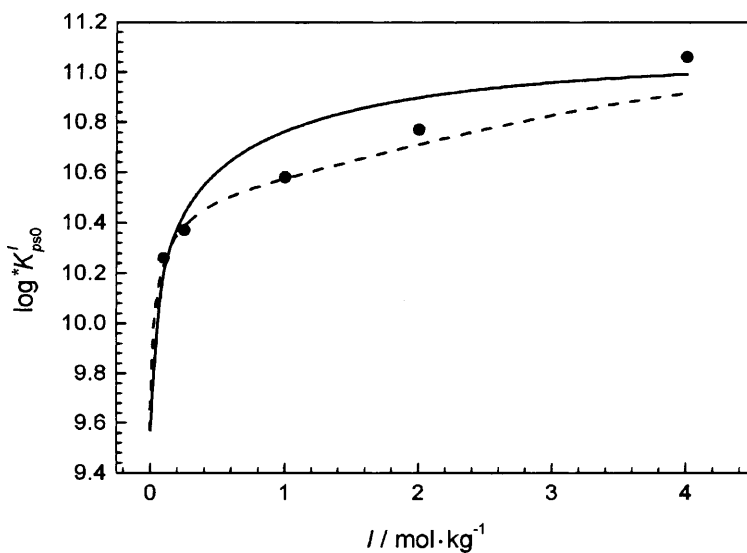


**Fig. 8.** Solubility constant of  $\text{La}_2(\text{CO}_3)_3 \cdot 8\text{H}_2\text{O}$  plotted vs. ionic strength at 298.15 K (inert electrolyte:  $\text{NaClO}_4$ );  $\log^* K_{ps0}^0 = 9.57 \pm 0.10$ ; ●: Nguyen *et al.* [7]; solid line: specific ion interaction theory [37]; dashed line: Pitzer model [38]

agreement of the model calculations with the experimental results. However, it is worth emphasizing that the calculations by means of the specific ion-interaction theory concur reasonably with the experimental data, such that the maximum deviation is less than  $0.2 \log^* K_{ps0}^0$  units in the range of  $0\text{--}4.0 \text{ mol} \cdot \text{kg}^{-1} \text{ NaClO}_4$

**Table 1.** Specific ion-interaction parameters

$\varepsilon(i, j)$	$\varepsilon(i, j; 298.15 \text{ K})$	$10^3 \partial \varepsilon(i, j) / \partial T$	Ref.
$\varepsilon(\text{H}^+, \text{ClO}_4^-)$	0.12	0.58	[10, 37]
$\varepsilon(\text{Na}^+, \text{ClO}_4^-)$	0.01	1.3	[10, 37]
$\varepsilon(\text{H}^+, \text{Cl}^-)$	0.12	-0.45	[37], this study
$\varepsilon(\text{Na}^+, \text{Cl}^-)$	0.03	0.46	[37], this study
$\varepsilon(\text{Na}^+, \text{OH}^-)$	0.04	0.27	[37], this study
$\varepsilon(\text{Na}^+, \text{HCO}_3^-)$	0.00	—	[37]
$\varepsilon(\text{Na}^+, \text{CO}_3^{2-})$	-0.06	—	[37]
$\varepsilon(\text{Ca}^{2+}, \text{ClO}_4^-)$	0.27	0.40	[37], this study
$\varepsilon(\text{Ca}^{2+}, \text{Cl}^-)$	0.14	-0.24	[45], this study
$\varepsilon(\text{Zn}^{2+}, \text{ClO}_4^-)$	0.36	0.40	[10, 37]
$\varepsilon(\text{Cu}^{2+}, \text{ClO}_4^-)$	0.32	—	[37]
$\varepsilon(\text{Cd}^{2+}, \text{ClO}_4^-)$	0.33	—	this study
$\varepsilon(\text{La}^{3+}, \text{ClO}_4^-)$	0.47	—	[37]
$\varepsilon(\text{CO}_2(\text{aq}), \text{ClO}_4^-)$	-0.061	—	<sup>a</sup>
$\varepsilon(\text{CO}_2(\text{aq}), \text{Cl}^-)$	-0.04	—	<sup>a</sup>
$\varepsilon(\text{CO}_2(\text{aq}), \text{Na}^+)$	0.087	—	<sup>a</sup>

<sup>a</sup>  $\varepsilon(k, j) = 2\lambda(k, j)/\ln(10)$ , calculated from the corresponding *Pitzer* parameters taken from Ref. [51]

with regard to lanthanite (Fig. 8). The solubility of calcite in solutions containing up to  $6.2 \text{ mol} \cdot \text{kg}^{-1}$  NaCl agrees even better with analogous predictions (Fig. 7).

All *Pitzer* parameters necessary for the calculations in this work can be found in Ref. [51]. The additional binary and ternary interaction parameters for the system  $\text{La}(\text{ClO}_4)_3\text{--NaClO}_4$  are taken from *Kim and Frederick* [52, 53]. The binary *Pitzer* parameters for  $\text{Cd}(\text{ClO}_4)_2$  can be found in Ref. [52], and the ternary parameters for the system  $\text{Cd}(\text{ClO}_4)_2\text{--NaClO}_4$  have been given by *Gamsjäger et al.* [9]. Finally, the binary interaction coefficients for  $\text{Zn}(\text{ClO}_4)_2$  are taken from Ref. [38].

The relevant parameters for the specific ion-interaction theory are listed in Table 1. Our coefficients are consistent within the limits of uncertainty with the data tabulated by *Grenthe et al.* [37]. The coefficient  $\varepsilon(\text{Cd}^{2+}, \text{ClO}_4^-)$  has been obtained from a fit of Eq. (10) to experimental mean activity coefficients of aqueous solutions of  $\text{Cd}(\text{ClO}_4)_2$  reported by *Kálmán et al.* [54] in the range from 0 to  $2.0 \text{ mol} \cdot \text{kg}^{-1}$ . The parameters  $\partial \varepsilon(i, j) / \partial T$  have been derived by fitting Eq. (16) to the data for  ${}^\phi L$  of the corresponding strong electrolytes taken from the NBS tables [55] up to a molality of  $2.0 \text{ mol} \cdot \text{kg}^{-1}$ .

### Thermodynamic Properties of Transition Metal Carbonates

The temperature dependence of the solubility constant at infinite dilution can be expressed as

$$\log {}^*K_{ps0}^0(T) = -\frac{\Delta_{\text{sol}}H^\ominus(298.15)}{R\ln(10)} \cdot \frac{1}{T} + \frac{\Delta_{\text{sol}}S^\ominus(298.15)}{R\ln(10)} - \frac{1}{R\ln(10)} \left( \frac{1}{T} \int_{298.15}^T \Delta_{\text{sol}}C_p^\ominus dT - \int_{298.15}^T \frac{\Delta_{\text{sol}}C_p^\ominus}{T} dT \right) \quad (18)$$

where  $\Delta_{\text{sol}}H^{\ominus}(298.15)$  and  $\Delta_{\text{sol}}S^{\ominus}(298.15)$  refer to the standard enthalpy and the standard entropy of solution, respectively. The symbol  $\Delta_{\text{sol}}C_p^{\ominus}$  denotes the change of the heat capacity for the reaction of Eq. (1). In general,  $\Delta_{\text{sol}}H^{\ominus}(298.15)$  as well as  $\Delta_{\text{sol}}S^{\ominus}(298.15)$  can be obtained from a fit of Eq. (18) to experimental data determined at various temperatures. If a suitable thermodynamic model, including the auxiliary data for all species involved in the solid-solute phase equilibrium, is available, the standard enthalpy of formation and the standard entropy of the solid compound can be derived from  $\Delta_{\text{sol}}H^{\ominus}(298.15)$  and  $\Delta_{\text{sol}}S^{\ominus}(298.15)$ . When the standard entropy of the solid carbonate is well-known from low-temperature heat capacity measurements, solubility data are a reliable source for the standard enthalpy of formation of the solid phase. The thermodynamic properties of transition metal carbonates investigated so far are summarized in Table 2, and the auxiliary data for the respective metal ions are listed in Table 3 (all uncertainties in this work correspond to  $2\sigma$ ). The present set of thermodynamic constants can be regarded as an extension of the thermodynamic model published previously by

**Table 2.** Thermodynamic properties of relevant mineral phases,  $T = 298.15 \text{ K}$

Mineral	Formula	$\Delta_f H^{\ominus}/\text{kJ} \cdot \text{mol}^{-1}$	$S^{\ominus}/\text{J} \cdot \text{mol}^{-1} \cdot \text{K}^{-1}$	$\Delta_f G^{\ominus}/\text{kJ} \cdot \text{mol}^{-1}$
Otavite	$\text{CdCO}_3$	$-752.1 \pm 0.8^a$	$103.9 \pm 0.2^b$	$-674.2 \pm 0.8^a$
Smithsonite	$\text{ZnCO}_3$	$-818.9 \pm 0.6^c$	$81.2 \pm 0.2^d$	$-737.3 \pm 0.6^c$
Hydrozincite	$\text{Zn}_5(\text{OH})_6(\text{CO}_3)_2$	$-3584 \pm 15^e$	$436 \pm 50^e$	$-3164.6 \pm 3.0^e$
Zincite	$\text{ZnO}$	$-350.46 \pm 0.27^f$	$43.65 \pm 0.40^f$	$-320.48 \pm 0.30^f$
Malachite	$\text{Cu}_2(\text{OH})_2\text{CO}_3$	$-1067.1 \pm 3.4^g$	$166.3 \pm 2.5^h$	$-903.3 \pm 1.2^g$
Azurite	$\text{Cu}_3(\text{OH})_2(\text{CO}_3)_2$	$-1675.1 \pm 5.1^g$	$254.4 \pm 3.8^h$	$-1434.2 \pm 1.8^g$
Tenorite	$\text{CuO}$	$-156.1 \pm 2.1^i$	$42.6 \pm 0.4^i$	$-128.3 \pm 2.1^i$
Siderite	$\text{FeCO}_3$	$-752.0 \pm 1.2^k$	$95.47 \pm 0.15^l$	$-678.9 \pm 1.2^k$

<sup>a</sup> Gamsjäger *et al.* [9]; <sup>b</sup> Archer [29]; <sup>c</sup> Preis *et al.* [10]; <sup>d</sup> Robie *et al.* [28]; <sup>e</sup> Preis and Gamsjäger [11]; <sup>f</sup> CODATA [56]; <sup>g</sup> Preis and Gamsjäger [57]; <sup>h</sup> Kiseleva *et al.* [19]; <sup>i</sup> JANAF tables [69]; <sup>k</sup> Preis and Gamsjäger [76]; <sup>l</sup> Robie *et al.* [27]

**Table 3.** Thermodynamic properties of aqueous species,  $T = 298.15 \text{ K}$

Species	$\Delta_f H^{\ominus}/\text{kJ} \cdot \text{mol}^{-1}$	$S^{\ominus}/\text{J} \cdot \text{mol}^{-1} \cdot \text{K}^{-1}$	$\Delta_f G^{\ominus}/\text{kJ} \cdot \text{mol}^{-1}$
$\text{Cd}^{2+}$	$-75.92 \pm 0.60^a$	$-72.8 \pm 1.5^a$	$-77.73 \pm 0.60^a$
$\text{Zn}^{2+}$	$-153.39 \pm 0.20^a$	$-109.8 \pm 0.5^a$	$-147.20 \pm 0.20^a$
$\text{ZnHCO}_3^+$	$-839.8 \pm 5.3^b$	$28 \pm 17^b$	$-742.2 \pm 5.3^b$
$\text{Cu}^{2+}$	$64.9 \pm 1.0^a$	$-98 \pm 4^a$	$65.0 \pm 0.1^a$
$\text{CuHCO}_3^+$	$-598.8 \pm 5.3^b$	$129 \pm 17^b$	$-533.9 \pm 5.3^b$
$\text{CuCO}_3(\text{aq})$	—	—	$-501.3 \pm 0.6^c$
$\text{Cu}(\text{CO}_3)_2^{2-}$	—	—	$-1046.9 \pm 0.6^c$
$\text{Fe}^{2+}$	$-90.0 \pm 0.5^d$	$-101.6 \pm 3.7^d$	$-90.5 \pm 1.0^d$
$\text{FeCO}_3(\text{aq})$	—	—	$-648.7 \pm 1.6^e$
$\text{Fe}(\text{CO}_3)_2^{2-}$	—	—	$-1186.9 \pm 1.6^e$

<sup>a</sup> CODATA [56]; <sup>b</sup> Bauman [58]; <sup>c</sup> Baes and Mesmer [59]; <sup>d</sup> Parker and Khodakovskii [72]; <sup>e</sup> Bruno *et al.* [75]

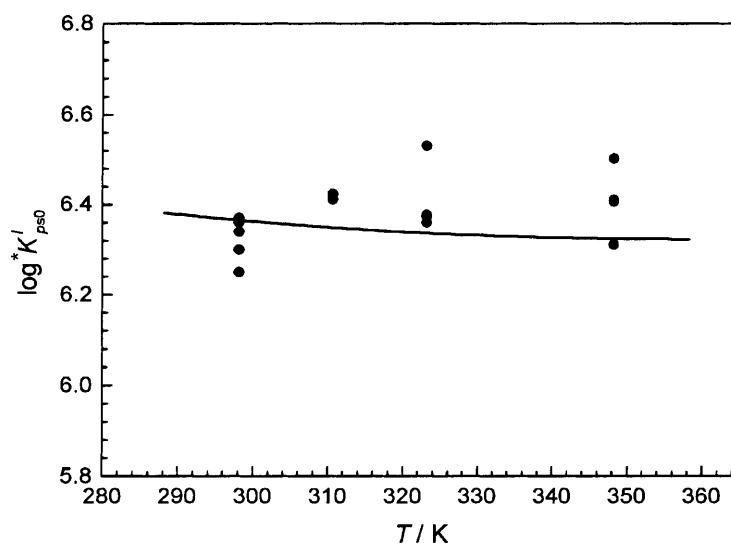
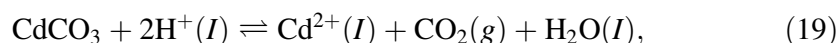


Fig. 9. Solubility constant of  $\text{CdCO}_3$  plotted vs. temperature,  $I = 1.00 \text{ mol} \cdot \text{kg}^{-1} \text{ NaClO}_4$ ; ●: experimental data [9]; solid line: Davies approximation [36]

Königsberger *et al.* [51]. It is worth mentioning that all auxiliary data are consistent with the CODATA key values for thermodynamics [56].

#### Cadmium carbonate

According to the dissolution reaction



the solubility constant of otavite reads

$$\log {}^*K_{ps0}^I = \log([\text{Cd}^{2+}]p(\text{CO}_2)) + 2p[H]. \quad (20)$$

As can be seen from Fig. 9, the solubility constant is independent of temperature within the limits of experimental error, leading to a vanishing enthalpy of solution  $\Delta_{\text{sol}}H^\ominus(298.15) = (-3.2 \pm 3.4) \approx 0 \text{ kJ} \cdot \text{mol}^{-1}$ . The solubility constant of otavite at 298.15 K concurs well with the results reported by Gamsjäger *et al.* [4] and Stipp *et al.* [60]. The standard entropy of otavite listed in Table 2 is based on low-temperature measurements of the heat capacity from 4.5 to 350 K [29]. A direct determination of the enthalpy of formation by using a calorimetric method has been reported in the literature [15]. These original data were evaluated by Wagman *et al.* [55], leading to  $\Delta_f H^\ominus(\text{CdCO}_3) = -750.6 \text{ kJ} \cdot \text{mol}^{-1}$ . However, this result has been criticized recently by Archer [29, 61]. Thus, measuring the temperature dependence of the solubility seems to yield the most reliable value for  $\Delta_f H^\ominus(\text{CdCO}_3)$ .

#### Zinc carbonates

The variations of the solubility constants of smithsonite ( $\text{ZnCO}_3$ ) and hydrozincite ( $\text{Zn}_5(\text{OH})_6(\text{CO}_3)_2$ ) with temperature at  $I = 1.00 \text{ mol} \cdot \text{kg}^{-1} \text{ NaClO}_4$  are depicted

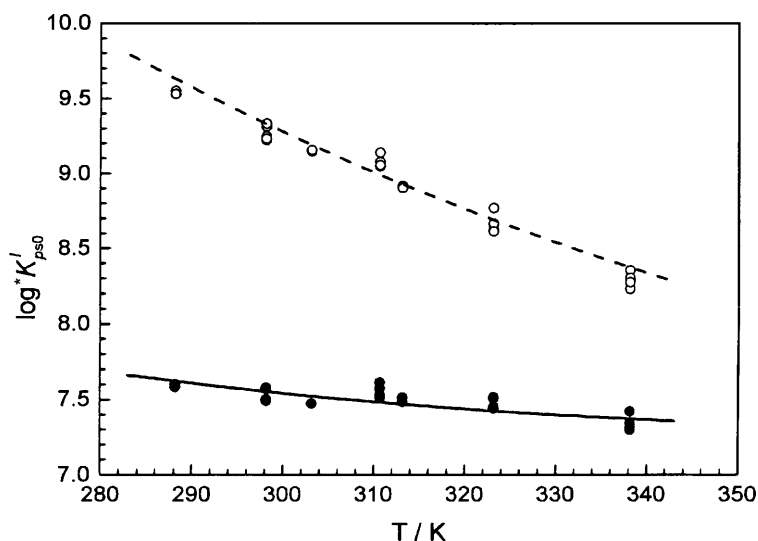
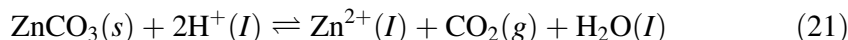


**Fig. 10.** Solubility constants of zinc carbonates plotted vs. temperature,  $I = 1.00 \text{ mol} \cdot \text{kg}^{-1} \text{ NaClO}_4$ ; experimental data: ●:  $\text{ZnCO}_3$  [10], ○:  $\text{Zn}_5(\text{OH})_6(\text{CO}_3)_2$  [11]; model calculations using the specific ion-interaction theory [37]: solid line:  $\text{ZnCO}_3$ , dashed line:  $\text{Zn}_5(\text{OH})_6(\text{CO}_3)_2$

in Fig. 10. The corresponding dissolution reactions can be written as



and

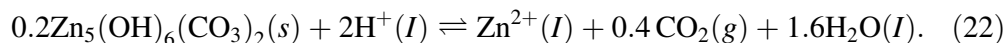
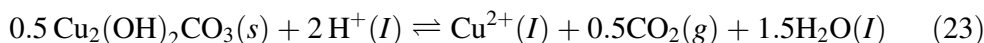


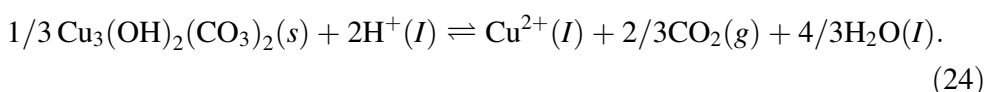
Figure 10 reveals that hydrozincite shows a pronounced dependence of the solubility constant on temperature in contrast to the neutral transition metal carbonate  $\text{ZnCO}_3$ . In the case of smithsonite, our solubility constants coincide satisfactorily with those given by *Smith* [62], *Schindler et al.* [6], and *Reiterer* [63]. The standard entropy was derived from low-temperature measurements of the heat capacity by *Robie et al.* [28]. The enthalpy of solution was found to be consistent with the heat of decomposition obtained from DSC experiments [10]. Our enthalpy of formation (Table 2) agrees well with  $\Delta_f H^\ominus(\text{ZnCO}_3) = -817 \text{ kJ} \cdot \text{mol}^{-1}$  estimated from the decarbonation pressure at elevated temperatures [25]. The standard enthalpy of formation  $\Delta_f H^\ominus(\text{ZnCO}_3) = -814.9 \text{ kJ} \cdot \text{mol}^{-1}$ , based on new auxiliary data and reported by *Roth and Chall* [16], deviates significantly from the value given in Table 2. The solubility constant of hydrozincite at 298.15 K is in close agreement with that published by *Schindler et al.* [6] and *Alwan and Williams* [64]. The standard *Gibbs* free energy of formation of hydrozincite coincides remarkably well with the results of *emf* measurements carried out by *Mercy et al.* [14]. The standard entropy of hydrozincite has not yet been determined directly by low-temperature measurements of the heat capacity. Thus, both the standard enthalpy of formation and the standard entropy listed in Table 2 are based on solubility measurements as a function of temperature [11].

### Copper carbonates

The dissolution reactions for the copper carbonates malachite ( $\text{Cu}_2(\text{OH})_2\text{CO}_3$ ) and azurite ( $\text{Cu}_3(\text{OH})_2(\text{CO}_3)_2$ ) read



and



The respective solubility constants, plotted as a function of temperature in Fig. 11, were found to be of the same order of magnitude. The temperature dependence of the solubility of  $\text{Cu}_2(\text{OH})_2\text{CO}_3$  seems to be somewhat more pronounced than that of  $\text{Cu}_3(\text{OH})_2(\text{CO}_3)_2$ .

The solubility constants agree satisfactorily with those obtained by *Free* [65], *Silman* [66], *Schindler et al.* [5], and *Symes and Kester* [67]. The standard entropies of malachite and azurite selected by *Robie and Hemingway* [68] are based on low-temperature measurements of the heat capacity [19]. Both solution and drop calorimetry were applied to determine the standard enthalpies of formation of malachite and azurite, leading to  $\Delta_f H^\ominus(\text{Cu}_2(\text{OH})_2\text{CO}_3) = -1054.0 \text{ kJ} \cdot \text{mol}^{-1}$  [18] and  $\Delta_f H^\ominus(\text{Cu}_3(\text{OH})_2(\text{CO}_3)_2) = -1632.2 \text{ kJ} \cdot \text{mol}^{-1}$  [17, 19]. These values were finally adopted by *Robie and Hemingway* [68]. According to this set of thermodynamic data, the equilibrium partial pressure of carbon dioxide for the coexistence of malachite and tenorite ( $\text{CuO}$ ) in aqueous media at 323.15 K should amount to 3.1 bar. However, by bubbling  $\text{CO}_2$  gas through an aqueous suspension of copper oxide it was possible to transform tenorite into pure malachite at

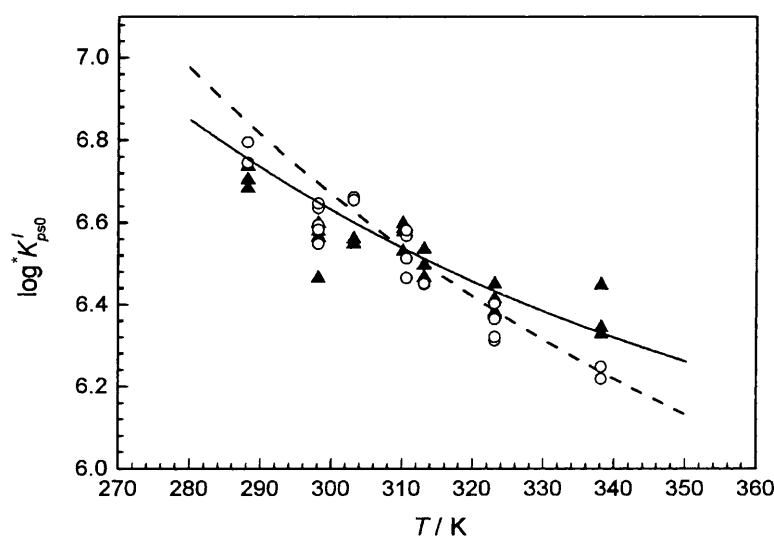


**Fig. 11.** Solubility constants of copper carbonates plotted vs. temperature,  $I = 1.00 \text{ mol} \cdot \text{kg}^{-1}$   $\text{NaClO}_4$ ; experimental data:  $\blacktriangle$ :  $\text{Cu}_3(\text{OH})_2(\text{CO}_3)_2$  [57],  $\circ$ :  $\text{Cu}_2(\text{OH})_2\text{CO}_3$  [57]; model calculations using the specific ion-interaction theory [37]: solid line:  $\text{Cu}_3(\text{OH})_2(\text{CO}_3)_2$ , dashed line:  $\text{Cu}_2(\text{OH})_2\text{CO}_3$

$p(\text{CO}_2) = 0.84$  bar and  $T = 323.15$  K. This observation clearly disproves the prediction based on the values listed in Ref. [68]. The thermodynamic data for CuO are consistent with the values of the JANAF tables [69] and are regarded to be fairly reliable. Thus, the thermodynamic properties of malachite and azurite were reinvestigated by performing solubility measurements as a function of temperature between 288.15 and 338.15 K and constant ionic strength ( $I = 1.00 \text{ mol} \cdot \text{kg}^{-1} \text{ NaClO}_4$ ) [57]. The results of these solubility measurements confirm the values for the standard entropies determined by *Kiseleva et al.* [19], whereas revised values for  $\Delta_f H^\ominus$  of both malachite and azurite are presented in Table 2.

### Iron(II) carbonate

Whereas solubility data for siderite ( $\text{FeCO}_3$ ) coincide remarkably well [70], a tremendous controversy occurs in literature with respect to the enthalpy of formation. *Wagman et al.* [55] as well as *Knacke et al.* [71] have selected  $-740.5 \text{ kJ} \cdot \text{mol}^{-1}$  for the enthalpy of formation, whereas  $\Delta_f H^\ominus(\text{FeCO}_3) = -755.9 \text{ kJ} \cdot \text{mol}^{-1}$  has been tabulated by *Robie and Hemingway* [68]. *Stubina and Toguri* [26] derived  $\Delta_f H^\ominus(\text{FeCO}_3) = -749 \text{ kJ} \cdot \text{mol}^{-1}$  from measurements of the decomposition pressure of siderite at elevated temperatures. *Chai and Navrotsky* [20] used a calorimetric method for the determination of this quantity and obtained  $\Delta_f H^\ominus(\text{FeCO}_3) = -750.6 \text{ kJ} \cdot \text{mol}^{-1}$ . The large difference in the values for the enthalpy of formation listed in data compilations seems to be caused by a discrepancy in the standard *Gibbs* free energy of formation of the iron(II) ion (NBS-tables [55]:  $\Delta_f G^\ominus(\text{Fe}^{2+}) = -78.9 \text{ kJ} \cdot \text{mol}^{-1}$ ; *Parker and Khodakovskii* [72]:  $\Delta_f G^\ominus(\text{Fe}^{2+}) = -90.53 \text{ kJ} \cdot \text{mol}^{-1}$ ). The thermodynamic properties of  $\text{Fe}^{2+}$

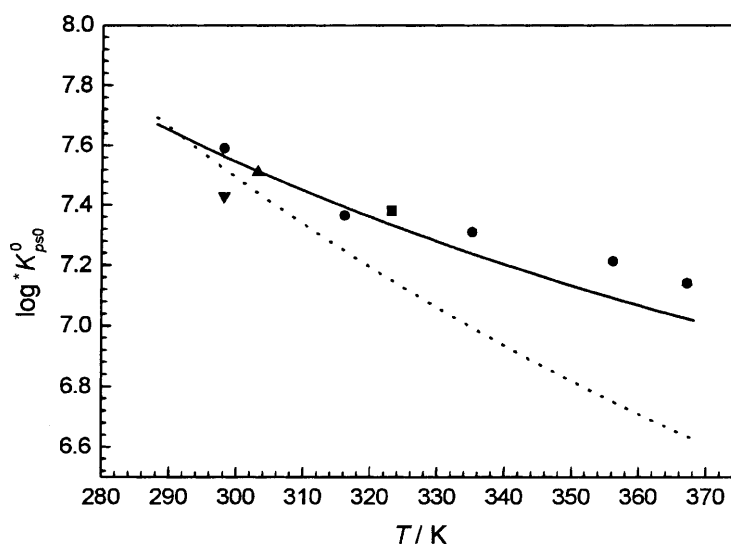


**Fig. 12.** Solubility constant of iron(II) carbonate plotted vs. temperature,  $I=0$ ; ▲: *Smith* [73]; ■: *Reiterer et al.* [63, 74]; ●: *Greenberg and Tomson* [77]; ▼: *Bruno et al.* [75]; solid line: *Preis and Gamsjäger* [76],  $\Delta_{\text{sol}} H^\ominus = (-17.3 \pm 1.2) \text{ kJ} \cdot \text{mol}^{-1}$ ; dashed line: *Wagman et al.* [55],  $\Delta_{\text{sol}} H^\ominus = -27.9 \text{ kJ} \cdot \text{mol}^{-1}$



recommended recently by *Parker and Khodakovskii* [72] were incorporated into our thermodynamic model in order to evaluate solubility data of siderite given by several literature sources. This critical evaluation led to an optimized value for the standard enthalpy of formation of siderite of  $\Delta_f H^\ominus(\text{FeCO}_3) = -752.0 \text{ kJ} \cdot \text{mol}^{-1}$ . The standard entropy of  $\text{FeCO}_3$  is taken from *Robie et al.* [27]. In contrast to the set of thermodynamic quantities listed in the NBS tables [55], the application of our thermodynamic model leads to a close agreement between the calculation of the temperature dependence of the solubility constant and various experimental data [73–75, 77]. Hence, Fig. 12 provides evidence for the reliability of both our value for  $\Delta_f H^\ominus(\text{FeCO}_3)$  and the  $\text{Fe}/\text{Fe}^{2+}$  standard potential ( $E_{\text{Fe}/\text{Fe}^{2+}}^\ominus = (-469.0 \pm 2.6) \text{ mV}$ ) recommended by *Parker and Khodakovskii* [72].

## Discussion and Conclusions

The most accurate technique for the determination of the standard entropy of a solid compound is the integration of low-temperature heat capacities. When such low-temperature measurements have not yet been published, the standard entropy is given by the entropy of solution obtained from solubility measurements at various temperatures.

Calorimetric methods as well as the evaluation of solubility measurements as a function of temperature yield the standard enthalpy of formation of metal carbonates. The enthalpies of solution of smithsonite [16], malachite [17, 18], and azurite [17] were studied by solution calorimetry where the respective mineral phase was dissolved in solutions of hydrochloric acid. Although the results show a high precision (low random errors), high systematic errors (low accuracy) might occur during the calorimetric measurements due to the evolution of unknown quantities of  $\text{CO}_2(\text{g})$ . The enthalpies of formation of malachite [19], azurite [19], and siderite [20] were determined by drop calorimetry. Especially, the decomposition experiments on malachite and azurite may suffer from systematic deviations, because the thermodynamic state of the microcrystalline metal oxide formed rapidly during the decarbonation might be poorly defined. In contrast to these direct methods it was shown in this work that a proper analysis of the temperature dependence of solubility constants yields the enthalpy of solution of sparingly-soluble carbonates. Obviously, the precision (absence of random error) of our equilibrium approach is expected to be much lower compared to the calorimetric methods. The evaluation of the temperature dependence of solubility data, however, avoids systematic errors, leading to a fairly high accuracy. Therefore, the enthalpy of solution was obtained with an estimated uncertainty of  $\pm 3 \text{ kJ} \cdot \text{mol}^{-1}$  per mole dissolved metal cation as summarized in Table 4. Using appropriate auxiliary data, the standard enthalpy of formation can be easily derived from the enthalpy of solution. All thermodynamic data derived in this work are consistent with the CODATA key values of thermodynamics [56]. The *Davies* approximation, the specific ion-interaction theory, and the *Pitzer* concept were used for the extrapolation of the solubility constants to zero ionic strength in order to obtain standard thermodynamic properties valid for infinite dilution. This procedure enables the simultaneous evaluation of solubility experiments performed in different ionic media (solvents) at various temperatures. Finally, from Table 4 it

**Table 4.** Solubility constants and enthalpies of solution at  $T=298.15$  K and  $I=0$  for relevant transition metal carbonates

Mineral	$\log^* K_{ps0}^0$	Dissolution reaction	$\Delta_{\text{sol}} H^\ominus / \text{kJ} \cdot \text{mol}^{-1}$
Otavite	6.14	$\text{CdCO}_3(\text{s}) + 2\text{H}^+(\text{aq}) \rightarrow \text{Cd}^{2+}(\text{aq}) + \text{CO}_2(\text{g}) + \text{H}_2\text{O}(\text{l})$	−3.2
Smithsonite	7.25	$\text{ZnCO}_3(\text{s}) + 2\text{H}^+(\text{aq}) \rightarrow \text{Zn}^{2+}(\text{aq}) + \text{CO}_2(\text{g}) + \text{H}_2\text{O}(\text{l})$	−13.8
Hydrozincite	9.00	$0.2\text{Zn}_5(\text{OH})_6(\text{CO}_3)_2(\text{s}) + 2\text{H}^+(\text{aq}) \rightarrow$ $\text{Zn}^{2+}(\text{aq}) + 0.4 \text{CO}_2(\text{g}) + 1.6 \text{H}_2\text{O}(\text{l})$	−51.3
Malachite	6.34	$0.5\text{Cu}_2(\text{OH})_2\text{CO}_3(\text{s}) + 2\text{H}^+(\text{aq}) \rightarrow$ $\text{Cu}^{2+}(\text{aq}) + 0.5 \text{CO}_2(\text{g}) + 1.5 \text{H}_2\text{O}(\text{l})$	−27.1
Azurite	6.30	$2/3\text{Cu}_3(\text{OH})_2(\text{CO}_3)_2(\text{s}) + 2\text{H}^+(\text{aq}) \rightarrow$ $\text{Cu}^{2+}(\text{aq}) + 2/3\text{CO}_2(\text{g}) + 4/3\text{H}_2\text{O}(\text{l})$	−20.2
Siderite	7.56	$\text{FeCO}_3(\text{s}) + 2\text{H}^+(\text{aq}) \rightarrow \text{Fe}^{2+}(\text{aq}) + \text{CO}_2(\text{g}) + \text{H}_2\text{O}(\text{l})$	−17.3

can be concluded that the temperature dependence of the solubility of basic transition metal carbonates is more pronounced than that of neutral carbonates, *i.e.* the enthalpy of solution becomes more negative when the ratio  $n(\text{OH})/n(\text{CO}_3)$  in the solid mineral increases.

## References

- [1] Stumm W, Morgan JJ (1996) Aquatic Chemistry 3rd edn. Wiley, New York
- [2] Eary LE (1999) Appl Geochem **14**: 963
- [3] Grauer R (1997) Solubility Limitations: An “Old Timer’s” view. In: Grenthe I, Puigdomenech I (eds) Modelling in Aquatic Chemistry. OECD NEA, Paris, pp 131–152
- [4] Gamsjäger H, Stuber HU, Schindler P (1965) Helv Chim Acta **48**: 723
- [5] Schindler P, Reinert M, Gamsjäger H (1968) Helv Chim Acta **51**: 1845
- [6] Schindler P, Reinert M, Gamsjäger H (1969) Helv Chim Acta **52**: 2327
- [7] Nguyen AM, Königsberger E, Marhold H, Gamsjäger H (1993) Monatsh Chem **124**: 1011
- [8] Gamsjäger H, Marhold H, Königsberger E, Tsai YJ, Kolmer H (1995) Z Naturforsch **50 a**: 59
- [9] Gamsjäger H, Preis W, Königsberger E, Magalhães MC, Brandão P (1999) J Solution Chem **28**: 717
- [10] Preis W, Königsberger E, Gamsjäger H (2000) J Solution Chem **29**: 605
- [11] Preis W, Gamsjäger H (2001) J Chem Thermodynamics (in press)
- [12] Rock PA, Casey WH, McBeath MK, Wallin EM (1994) Geochim Cosmochim Acta **58**: 4281
- [13] Casey WH, Rock PA, Chung JB, Walling EM, McBeath MK (1996) Amer J Sci **296**: 1
- [14] Mercy MA, Rock PA, Casey WH, Mokarram MM (1998) Amer Mineral **83**: 739
- [15] Thomsen J (1883) Thermochemische Untersuchungen, vol 3, Metals. Johann Ambrosius, Leipzig
- [16] Roth WA, Chall P (1928) Z Elektrochem **34**: 185
- [17] Roth WA, Berendt H, Wirths G (1941) Z Elektrochem **47**: 185
- [18] Richardson DW, Brown RR (1974) U S Bur Mines Rep Inv **7851**: 1–5
- [19] Kiseleva IA, Ogorodova LP, Melchakova LV, Bisengalieva MR, Becturganov NS (1992) Phys Chem Minerals **19**: 322
- [20] Chai L, Navrotsky A (1994) Amer Mineral **79**: 921
- [21] Chai L, Navrotsky A (1996) Geochim Cosmochim Acta **60**: 4377
- [22] Navrotsky A, Rapp RP, Smelik E, Burnley P, Circone S, Chai L, Bose K, Westrich HR (1994) Amer Mineral **79**: 1099

- [23] Kiseleva IA, Kotelnikov AR, Martynov KV, Ogorodova LP, Kabalov JK (1994) *Phys Chem Minerals* **21**: 392
- [24] Casey WH, Chai L, Navrotsky A, Rock PA (1996) *Geochim Cosmochim Acta* **60**: 933
- [25] Haselton HT, Goldsmith JR (1987) *Geochim Cosmochim Acta* **51**: 261
- [26] Stubina NM, Toguri JM (1989) *ISS Transactions* **10**: 87
- [27] Robie RA, Haselton HT, Hemingway BS (1984) *Amer Mineral* **69**: 349
- [28] Robie RA, Haselton HT, Hemingway BS (1989) *J Chem Thermodynamics* **21**: 743
- [29] Archer DG (1996) *J Chem Eng Data* **41**: 852
- [30] Schindler P (1963) *Chimia* **17**: 313
- [31] Heindl R, Gamsjäger H (1977) *Monatsh Chem* **108**: 1365
- [32] Gamsjäger H, Reiterer F (1979) *Environment International* **2**: 419
- [33] Königsberger E, Eriksson G (1995) *CALPHAD* **19**: 207
- [34] Robinson RA, Stokes RH (1959) *Electrolyte Solutions*, 2nd edn. Butterworths, London
- [35] Lewis GN, Randall M (1961) *Thermodynamics*. McGraw-Hill, New York, NY (revised by Pitzer KS, Brewer L)
- [36] Davies CW (1962) *Ion Association*. Butterworths, London
- [37] Grenthe I, Plyasunov AV, Spahiu K (1997) Estimations of medium effects on thermodynamic data. In: Grenthe I, Puigdomenech I (eds) *Modelling in Aquatic Chemistry*. OECD NEA, Paris, pp 325–426
- [38] Pitzer KS (1991) Ion interaction approach: Theory and data correlation. In: Pitzer KS (ed) *Activity Coefficients in Electrolyte Solutions*, 2nd edn. CRC Press, Boca Raton, Florida, pp 76–153
- [39] Brønsted JN (1922) *J Am Chem Soc* **44**: 877
- [40] Brønsted JN (1922) *J Am Chem Soc* **44**: 938
- [41] Guggenheim EA (1935) *Phil Mag* **19**: 588
- [42] Scatchard G (1936) *Chem Rev* **19**: 309
- [43] Eriksson G, Hack K (1990) *Metall Trans* **21 B**: 1013
- [44] Goldberg RN (1981) *J Phys Chem Ref Data* **10**: 1
- [45] Fischer R, Byé J (1964) *Bull Soc Chim*, pp 2920–2929
- [46] Carpeni G, Boitard E, Pilard R, Poize S, Sabiani N (1973) *J Chim Phys* **69**: 1445
- [47] Kron I, Marshall SL, May PM, Hefter G, Königsberger E (1995) *Montsh Chem* **126**: 819
- [48] Sjöberg S, Höglund Y, Nordin A, Ingri N (1983) *Mar Chem* **13**: 35
- [49] Näsänen R, Meriläinen P (1960) *Suomen Kem* **B33**: 149
- [50] Wolf M, Breitskopf O, Puk R (1989) *Chem Geol* **76**: 291
- [51] Königsberger E, Königsberger L-C, Gamsjäger H (1999) *Geochim Cosmochim Acta* **63**: 3105
- [52] Kim H-T, Frederick Jr WJ (1988) *J Chem Eng Data* **33**: 177
- [53] Kim H-T, Frederick Jr WJ (1988) *J Chem Eng Data* **33**: 278
- [54] Kálmán E, Horn G, Schwabe K (1970) *Z Phys Chem* **244**: 106
- [55] Wagman DD, Evans WH, Parker VB, Schumm RH, Halow I, Bailey SM, Churney KL, Nuttall RL (1982) *J Phys Chem Ref Data* **11** (Suppl 2)
- [56] Cox JD, Wagman DD, Medvedev VA (1989) *CODATA Key Values for Thermodynamics*. Hemisphere Publishing Corporation, Washington, New York, London
- [57] Preis W, Gamsjäger H (2001) *J Chem Thermodynamics* (submitted)
- [58] Bauman Jr JE (1981) *U S Bur Mines Inf Circ* **8852**: 268
- [59] Baes CF, Mesmer RE (1976) *The Hydrolysis of Cations*. Wiley, New York
- [60] Stipp SL, Parks GA, Nordstrom DK, Leckie JO (1993) *Geochim Cosmochim Acta* **57**: 2699
- [61] Archer DG (1998) *J Phys Chem Ref Data* **27**: 915
- [62] Smith HJ (1918) *J Amer Chem Soc* **40**: 883
- [63] Reiterer F (1980) *Löslichkeitskonstanten und Freie Bildungsenthalpien neutraler Übergangsmetallcarbonate*. PhD Thesis, Montanuniversität Leoben, Austria
- [64] Alwan AK, Williams PA (1979) *Trans Met Chem* **4**: 128
- [65] Free RE (1908) *J Amer Chem Soc* **30**: 1366

- [66] Silman JFB (1958) PhD Thesis, Harvard University
- [67] Symes JL, Kester DR (1984) *Geochim Cosmochim Acta* **48**: 2219
- [68] Robie RA, Hemingway BS (1995) Thermodynamic properties of minerals and related substances at 298.15 K and 1 bar ( $10^5$  Pascals) pressure and at higher temperatures. US Geological Survey Bulletin 2131, Washington
- [69] Chase MW (1998) NIST-JANAF Thermochemical Tables, Part II, Cr-Zr 4th edn. American Chemical Society, Gaithersburg, Maryland
- [70] Grauer R (1994) Bereinigte Löslichkeitsprodukte von M(II)-Schwermetallcarbonaten. Paul Scherrer Institut, Internal Technical Report, TM-44-94-05, pp 1–35
- [71] Knacke O, Kubaschewski O, Hesselmann K (1991) Thermochemical Properties of Inorganic Substances, 2nd edn. Springer-Verlag, Verlag Stahleisen G.m.b.H., Berlin, Düsseldorf
- [72] Parker VB, Khodakovskii IL (1995) *J Phys Chem Ref Data* **24**: 1699
- [73] Smith HJ (1918) *J Amer Chem Soc* **40**: 879
- [74] Reiterer F, Johannes W, Gamsjäger H (1981) *Mikrochim Acta* **I**: 63
- [75] Bruno J, Wersin P, Stumm W (1992) *Geochim Cosmochim Acta* **56**: 1149
- [76] Preis W, Gamsjäger H (2001) Critical evaluation of solubility data: Enthalpy of formation of siderite. *Phys Chem Chem Phys* (in preparation)
- [77] Greenberg J, Tomson M (1992) *Appl Geochem* **7**: 185

*Received June 26, 2001. Accepted July 2, 2001*